Direct Numerical Simulations of Reacting Flows in Homogeneous Turbulence

Feng Gao and Edward E. O'Brien
Dept. of Mechanical Engineering, State University of New York, Stony Brook, NY 11794

A direct numerical simulation (DNS) code has been modified to investigate chemically reacting flows in a stationary, homogeneous turbulence. Single and multispecies reactions as well as complicated reaction schemes such as parallel/consecutive reactions are studied. The effects of some parameters are discussed. The numerical data are used to test a simple first-order closure model, proposed by Dutta and Tarbell (1989), for turbulent reacting flows. It is shown that the DNS technique provides us with an effective tool to isolate the effects of different parameters and is likely to be useful for proposing and testing closure models.

Introduction

Investigation of turbulent reacting flows has been an important area in turbulence research and has many applications in practical fields such as chemical engineering and combustion. Because of the chaotic nature of the problem, statistical descriptions of the turbulent fields are adopted. A major difficulty accompanying the statistical theory of turbulence is that when the governing equations are averaged to obtain the means, the equations become unclosed due to strongly nonlinear reactions and complicated velocity-scalar interactions. Traditionally, closure models are proposed that relate these unclosed terms to the resolved quantities (Dutta and Tarbell, 1989; Heeb and Brodkey, 1990).

Because of the difficulties encountered in conducting turbulent reacting flow experiments under controlled conditions, our knowledge about this area has been very limited, which therefore restricts the scope of proper closure proposals. In this situation, the recently developed direct numerical simulation (DNS) techniques provide an important alternative for the turbulent reacting flow research (for example, Riley et al., 1986). Advances in computer technology in the past two decades have made it possible to numerically simulate turbulent flows of moderate Reynolds numbers. Using this approach, all the significant scales in the turbulence fields are resolved explicitly so that no *ad hoc* assumptions are needed. Provided that the physical processes are accurately described by the Navier-Stokes equations and the scalar evolutions equations, this method provides a way to conduct experiments numerically, which has certain advantages over the traditional experimental approach. First, it provides information that is difficult to obtain experimentally, and second, the parameters, such as Schmidt number and Damköhler number, can be easily varied. The disadvantages of this method, however, are also obvious. The major one is the limitations on spatial and time scales that can be resolved.

Other authors have also employed DNS to investigate turbulent reacting flow problems (Givi and McMurtry, 1988; Leonard and Hill, 1989, 1990). In this article, a code, originally developed by Rogallo (1981) and later modified by Eswaran and Pope (1988a) to simulate stationary turbulence, has been extended to accommodate chemically reacting flows. Single- and multispecies reactions as well as single-step and multistep reactions are considered. The effects of some parameters, such as Damköhler number and initial length scale, are studied. Numerical experiments have been conducted to test the 3E/4E pure mixing asymptote closure models that were recently proposed by Dutta and Tarbell (1989).

Numerical Method

The program used in this study is the well established pseudospectral scheme and solves, for statistically homogeneous fields in the three-dimensional space, the incompressible Navier-Stokes equations as well as the scalar transport equations. It was developed originally by Rogallo (1981) for decaying turbulence and later modified by Eswaran and Pope (1988a) by forcing the large-scale velocity components (energy is added to the velocity components in $0 \leq k \leq K_F$ in the wave number

Current address of F. Gao: Center for Turbulence Research, Building 500, Stanford University, Stanford, CA 94305.

space) by Uhlenbeck-Ornstein processes to yield a statistically stationary flow field. It has been used to investigate the behavior of a nonreacting scalar in homogeneous stationary turbulence (Eswaran and Pope, 1988b).

In this research, the chemical reaction source terms are included in the scalar transport equations to deal with finite reaction rate reacting flow problems. It has been shown that the inclusion of these source terms does not impose additional numerical stability conditions (Gao, 1990), as will be described in the following. More detailed discussions can be found elsewhere (Rogallo, 1981; Eswaran and Pope, 1988a; Gao, 1990).

Pseudospectral scheme

The equations to be solved are:

$$\frac{\partial \vec{v}}{\partial t} + \vec{v} \cdot \nabla \vec{v} = \nu \nabla^2 \vec{v} - \nabla p + \vec{f} \tag{1}$$

$$\nabla \vec{v} = 0 \tag{2}$$

$$\frac{\partial \phi_i}{\partial t} + \vec{v} \cdot \nabla \phi_i = D_{\phi i} \nabla^2 \phi_i + S_i(\vec{\phi}), \tag{3}$$

where $vecv = (v_1, v_2, v_3) = (u, v, w)$ is the velocity field; ν is the fluid viscosity; $\vec{f} = (f_1, f_2, f_3)$ is the external force to maintain the turbulence energy; ϕ_i is the concentration of species i; and S_i is the reaction source term for species i.

The concerned field f (fields like u, v, w and ϕ_i) is represented by $f(j_1, j_2, j_3)$ on N^3 node points $(x_{j1}, y_{j2}, z_{j3}) = [(j_1 - 1)\Delta x, (j_2 - 1)\Delta x, (j_3 - 1)\Delta x]$ in the domain $(0, 2\pi; 0, 2\pi; 0, 2\pi)$, where $\Delta x = 2\pi/(N - 1)$. To employ efficient Fourier transform techniques, N is chosen to be 2^n. The time integration is carried out in the wave number space (k_1, k_2, k_3), which spans the integer grids in $[1 - (N/2), (N/2); 1 - (N/2), (N/2); 1 - (N/2), (N/2)]$, by a second-order Runge-Kutta scheme for the field components at each wave number (for each Fourier component) (Rogallo, 1981; Eswaran and Pope, 1988a). Field components in the wave number space $\tilde{f}(k_1, k_2, k_3)$ can be related to those in the real physical space by:

$$f(j_1,j_2,j_3) = \sum_{1-N/2}^{N/2} \sum_{1-N/2}^{N/2} \sum_{1-N/2}^{N/2} \tilde{f}(k_1,k_2,k_3) e^{i(k_1 x_{j1} + k_2 y_{j2} + k_3 z_{j3})}. \tag{4}$$

Substituting Eq. 4 into Eqs. 1 and 3, the evolution equations for the Fourier components can be written as:

$$\frac{\partial \tilde{v}_j}{\partial t} + \mathfrak{F}\left[u \frac{\partial v_j}{\partial x} + v \frac{\partial v_j}{\partial y} + w \frac{\partial v_j}{\partial z} \right] = -\nu k^2 \tilde{v}_j + \tilde{f}_j - i k_j \tilde{p}, \tag{5}$$

for a velocity component and

$$\frac{\partial \tilde{\phi}_j}{\partial t} + \mathfrak{F}\left[u \frac{\partial \phi_j}{\partial x} + v \frac{\partial \phi_j}{\partial y} + w \frac{\partial \phi_j}{\partial z} - S_j(\vec{\phi}) \right] = -D_\phi k^2 \tilde{\phi}_j, \tag{6}$$

for the concentration of species j, where $\mathfrak{F}[\bullet]$ indicates a Fourier transform of the bracketed quantities.

To evaluate the Fourier transform of terms $\vec{u} \cdot \nabla \phi$ efficiently, both $\vec{u}$ and $\nabla \phi$ are transformed back to the real space and the products are then transformed to the wave number space (Patterson and Orszag, 1971). Whenever multiplications in real space are performed, however, an error known as the aliasing error arises because of the finite periodicity of e^{ikx_j} in wave number space. Both phase shifting and truncation methods have been introduced to remove the aliasing errors for bilinear multiplication terms (Patterson and Orszag, 1971; Rogallo, 1981). To use this method for the solution of chemical reaction problems, the reaction terms should be no greater than power 2 to avoid more aliasing errors than those caused by the bilinear products (Gao, 1990).

More details about the pseudospectral method can be found in other references (such as Gottlieb and Orszag, 1977; Hussaini and Zang, 1987).

Data extraction

To extract useful data from the computation, the assumption of homogeneity is used. With this assumption, the ensemble average can be replaced by the space average.

In the spatial average, each grid point is considered as a sample in the ensemble. For example, if

$$f(j) = \sum_{k=1-N/2}^{N/2} \tilde{f}(k) e^{ikx_j} \text{ and } g(j) = \sum_{k=1-N/2}^{N/2} \tilde{g}(k) e^{ikx_j},$$

where $j = 1, 2, \ldots, N$. The statistics of f and g are then evaluated by:

$$\langle f \rangle = \frac{1}{N} \sum_{j=1}^{N} f(j) \text{ and } \langle fg \rangle = \frac{1}{N} \sum_{j=1}^{N} f(j) g(j) \text{ etc.},$$

where angle bracket represents the mean of a quantity.

Noting that $\langle e^{ikx} \rangle = \delta_{k0}$, and f and g are real, one obtains:

$$\langle f \rangle = \tilde{f}(0) \text{ and } \langle fg \rangle = \langle fg^* \rangle = \sum_{k=1-N/2}^{N/2} \tilde{f}(k) \tilde{g}^*(k) \text{ etc.},$$

where g^* is the conjugate of g. Hence, all the moments up to the second order can be calculated directly from the wave space quantities.

If the desired moment is of the third or higher orders, it is more efficient to transform all the related quantities back to real space to perform space average.

Besides the numerical scheme error, the major source of sampling error is the finite size of the sample space. As is well known, if

$$\langle A \rangle = \lim_{N \to \infty} \frac{1}{N} \sum_{i=1}^{N} A_i$$

and

$$\overline{A}_N = \frac{1}{N} \sum_{i=1}^{N} A_i,$$

$\overline{A}_N$ forms a near Gaussian random variable with mean $\langle A \rangle$

and standard deviation proportional to $1/N$, if N is large, that is,

$$E\left\{\left(\frac{1}{N}\sum_{i=1}^{N}A_i-\langle A\rangle\right)^2\right\}\propto\frac{1}{N}.$$

Here $E\{\bullet\}$ denotes the mean expected value of random variable $\bullet$.

Initial conditions

The initial fields are generated according to their spectrum. The randomness of the fields was imposed by introducing random phase.

For the velocity field, if the large-scale structures are enforced by artificial energy to yield a stationary turbulence field, the initial velocity field is not important because after a transient period, the field will lose its memory of the initial state. The final stationary state is determined by the forcing energy.

For scalar fields, the initial values can be generated by:

$$\tilde{\phi}(k)=\left(\frac{E_\phi(k)}{4\pi k^2}\right)^{1/2}e^{i\theta_\phi}$$

where

$$E_\phi(k)=\int\tilde{\phi}(k)\tilde{\phi}^*(k)dA(k).$$

The integration is over a sphere surface $|\vec{k}|=k$ in the wave number space, and θ_ϕ is a random number uniformly distributed on $(0, 2\pi)$.

To introduce the length scale information for the initial scalar field (narrow wave-length band), Eswaran and Pope (1988b) used a spike-shaped initial spectrum,

$$E_\phi(k,k_s)=\begin{cases}1 & \text{if } k_s-\frac{1}{2}\le k\le k_s+\frac{1}{2}\\ 0 & \text{otherwise}\end{cases}. \tag{7}$$

where k_s corresponds to the length scale l_s of the initial scalar field. The standard deviation of this scalar is normalized since

$$\langle(\phi-\langle\phi\rangle)(\phi-\langle\phi\rangle)\rangle=\int_{k_s-1/2}^{k_s+1/2}E_\phi(k)dk=1$$

This method is used in this research. A procedure is developed for using such spectra to generate two initial scalar fields with a prescribed correlation coefficient. Suppose

$$\tilde{\phi}_1(k)=\sqrt{\frac{E_\phi(k,k_{s1})}{4\pi k^2}}\,e^{i\theta_1(\vec{k})}\text{ and }\tilde{\phi}_2(k)=\sqrt{\frac{E_\phi(k,k_{s2})}{4\pi k^2}}\,e^{i\theta_2(\vec{k})}$$

it can be shown that

$$\overline{\phi_1\phi_2}=\int\frac{\sqrt{E_\phi(k,k_{s1})E_\phi(k,k_{k2})}}{4\pi k^2}\,e^{i(\theta_1-\theta_2)}d\vec{k}. \tag{8}$$

Several kinds of initial fields can be generated from Eq. 8. First, if θ_1 and θ_2 are independently generated random numbers, the correlation is zero, indicating ϕ_1 and ϕ_2 are not related to each other. Second, if θ_1 and θ_2 are generated equal to each other, but $E(k,k_{s1})$ and $E(k,k_{s2})$ are not overlapping ($|k_{s1}-k_{s2}|>1$), the correlation is also zero, meaning scalars with totally different length scales are not related either. Finally, if $\theta_1=\theta_2$ and $|k_{s1}-k_{s2}|=\alpha\le 1$, Eq. 8 leads to $\overline{\phi_1\phi_2}=1-\alpha$, which provides a way to generate initial scalar fields with a prescribed correlation coefficient.

In this article *sisj* and *sicj* represent different two scalar initial fields. The former indicates that θ_1 and θ_2 are independently generated random numbers, hence the correlation between the initial two scalar fields is zero, and the latter represents $\theta_1=\theta_2$ (correlated) cases. The first scalar is generated by $si(k_s=i)$ and the second one by *sj* or *cj*, as shown in Table 1. The *s1c1* case is for two identical initial scalar fields ($k_{s1}=k_{s2}$) with $\theta_1=\theta_2$, hence the correlation is one. In all two scalar initializations, both species are identically distributed at $t=0$, therefore the stoichiometry is unity.

Results and Discussions

The turbulent velocity field is calculated first. Since the velocity fields are forced by adding energy to the large scale, they reach the stationary states after a transient period (Eswaran and Pope, 1988a). The turbulence fields are characterized by three length scales (Hinze, 1975; Eswaran and Pope, 1988a).

Average integral scale:

$$l=\frac{\pi}{2u^2}\int_0^{k_{\max}}k^{-1}E(k)dk,$$

Kolmogorov scale:

$$\eta=\left(\frac{\nu^3}{\epsilon}\right)^{1/4}$$

Taylor microscale:

$$\lambda=\left(\frac{\epsilon}{15\nu u^2}\right)^{-1/2}.$$

These scales, along with the eddy-turnover time scale, l/u, and the Reynolds number based on the Taylor scale, Re_λ, are listed in Table 2.

The scalar fields are generated on the interval [0, 1] in composition space with various initial length scales and *pdf* shapes. The *pdfs* considered are of two types, the first is the "double-delta" type that has peaks at 0 and 1 (represented by "*pd*"), the other is bell-shaped centered at 0.5 (represented by "*pb*"). The initial scalar spectra are assumed spike-shaped centered at k_s. The initial scalar fields are characterized by two length scales.

Integral length scale:

$$l_\phi=\frac{\pi}{2\langle(\phi_f)^2\rangle}\int_0^{k_{\max}}k^{-1}E_\phi(k)dk,$$

Table 1. Specifications of Initial Scalar Fields

PDF	Cases	Mesh Size	k_s	l_ϕ/l	λ_ϕ/λ
v1pd	pds1	64^3	1	1.019	1.016
	pds2	64^3	2	0.536	0.749
	pds4	64^3	4	0.280	0.538
v1pb	pbs2	64^3	2	0.646	1.859
v2pd	pds2	64^3	2	0.373	0.519
v2pb	pbs2	64^3	2	0.442	1.267
v3pb	pbs2	32^3	2	0.577	1.367
	pbs3	32^3	3	0.385	0.977
	pbc2	32^3	2.5	0.503	1.188
	pbc3	32^3	2.8	0.444	1.068
v4pd	pds2	32^3	2	0.429	0.668
	pds3	32^3	3	0.293	0.545
v5pb	pbs1	32^3	1	*	0.862
	pbs2	32^3	2	*	0.605

*The quantity has not been calculated in the original simulation.

Scalar dissipation scale:

$$\lambda_\phi = \left[\frac{\langle \epsilon_\phi \rangle}{6D_\phi \langle (\phi_f)^2 \rangle} \right]^{-1/2},$$

where ϕ_f is the fluctuation of scalar concentration ϕ. In Table 1, the column "PDF" indicates the initial shape of the scalar PDF combined with the associated velocity field; the initial scalar fields are further specified by the initial length scale (represented by k_s) and coded in the column "Cases."

The numerical data are tested first against some known results. Then, they are used to investigate the effects of several parameters such as the initial length scale. Finally, they are employed to examine a simple closure model proposed by Dutta and Tarbell (1989). It is shown that this code is capable of handling different types of chemical schemes as long as the reactions involved are second order or lower. The data shown are selected from a broader set that is available (Gao, 1990).

Test of the numerical code

Here we consider simple reactions, by which we mean one-step reactions of the following type:

$$A + B \xrightarrow{c_1} \text{Products.} \tag{9}$$

The reaction source term can be written as $-c_1\phi_a\phi_b$.

If $B = 0$ or $B = A$, it becomes a single scalar reaction,

$$nA \xrightarrow{c_1} \text{Products,} \tag{10}$$

where n equals 1 or 2 and is referred to as the order of reaction hereafter.

Table 2. Specifications of Velocity Fields

Vel. Field	Mesh Points	η	l	λ	l/u	Re_λ
v1	64^3	0.0429	1.2156	0.5754	0.6012	46.54
v2	64^3	0.0607	1.7773	0.8841	1.1457	54.86
v3	32^3	0.0874	1.3585	0.8006	2.0057	21.69
v4	32^3	0.0818	1.5802	0.9250	1.7728	32.98
v5	32^3	0.1248	2.0134	1.2988	3.7358	28.00

In the following discussions, we will use the Damköhler number *Da*, which is the ratio of the turbulence time scale l/u to the chemical reaction time scale τ_c representing reaction rate ($= 1/c_1\sqrt{\langle\phi_{a0}\rangle\langle\phi_{b0}\rangle}$ in the case of reaction 9, where $\langle\phi_{a0}\rangle$ and $\langle\phi_{b0}\rangle$ are the initial means of scalars *a* and *b*). For large Damköhler numbers, the turbulent mixing time scale is much greater than the scalar reaction time scale, and the situation becomes diffusion-limited because reactions simply cannot happen between unmixed species. Hence, the time scale of the whole process is determined largely by the mixing time scale. On the other hand, for low Damköhler numbers, the time scale is more likely to be determined by the reaction rate.

There are several cases where the performance of the numerical method can be tested. One of these cases is the first-order reactions for which some analytical results have been derived (Corrsin, 1958; O'Brien, 1960). Another test is performed on one-step, two-species reactions, where some qualitative features can be deduced readily.

Single-Scalar Reactions. It has been shown that the evolution of a scalar field under first-order chemical reaction is equivalent to that of its corresponding nonreacting value in the same flow field multiplied by an exponential decaying factor, $e^{-c_1 t}$. This is an ideal case for testing the performance of the numerical code. It has been shown that the numerical results for scalar mean, variance, and Taylor microscale are almost identical to those predicted by the theory (Gao, 1990).

For second-order reactions, the reaction rate becomes very slow after a certain transient period, hence the governing equation for the evolution of the scalar can be linearized (Gao, 1990). It is, therefore, concluded that after the initial period, linear behavior will be exhibited, similar to that shown in the first-order reaction case. The numerical results agree with this (Gao, 1990).

Two-Species Cases. We define the correlation coefficient γ as:

$$\gamma = \frac{\langle \phi_{af}\phi_{bf} \rangle}{\sqrt{\langle \phi_{af}^2 \rangle \langle \phi_{bf}^2 \rangle}},$$

where the subscript f denotes the fluctuation of the scalar concentration (for example, $\phi_{af} = \phi_a - \langle\phi_a\rangle$). It is a measure of the degree of engagement between two species ϕ_a and ϕ_b.

If $c_1 = 0$, two species evolve independently; therefore, there should be little change in the correlation coefficient and the scalar means are constant. The numerical results (not shown) reproduce this behavior. When the chemical reaction is turned on, these two species interact more and more at a rate depending on the Damköhler number *Da*. The correlation coefficient eventually tends to -1, an indication of perfect correlation. The numerical results show such a trend (Figure 1).

Effects of some parameters

The effects of initial length scale, Damköhler number and initial correlation have been considered. Some of the results are summarized below.

For both second-order, single-scalar and one step, two-species reaction cases, it has been observed that the evolution of the scalar means is affected little by the initial length scale (Figures 2 and 3). At $Da = 1$, the variances of both scalars

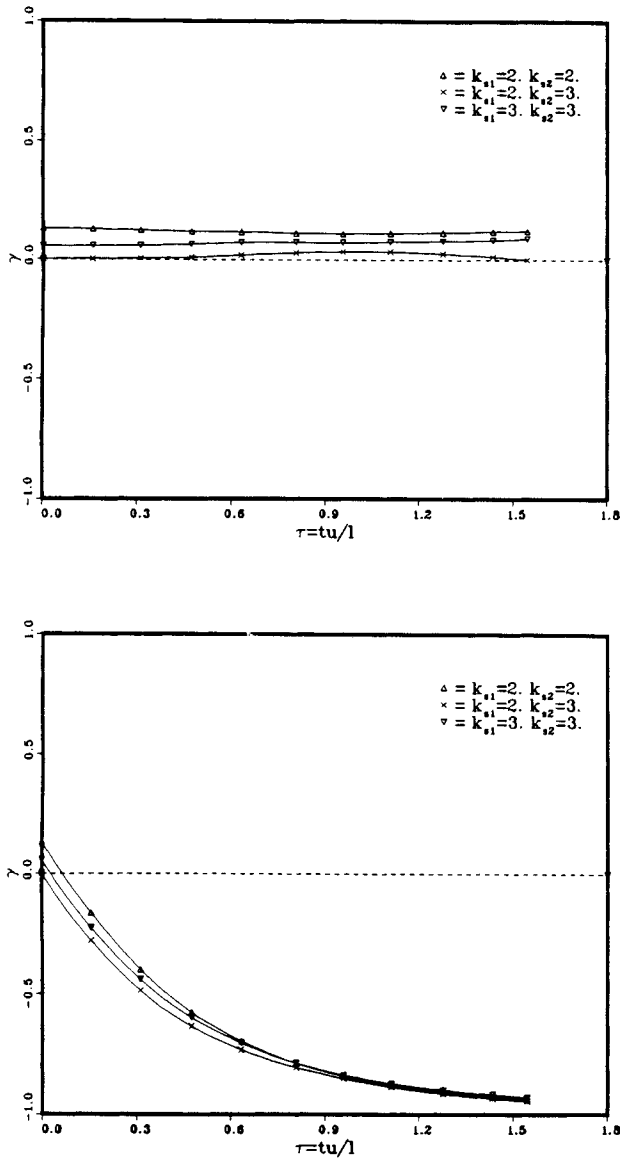

Figure 1. Evolution of γ for various initial scalar fields.

Da = 0.0 (upper); *Da* = 1.0 (lower); Run *v3pd*.

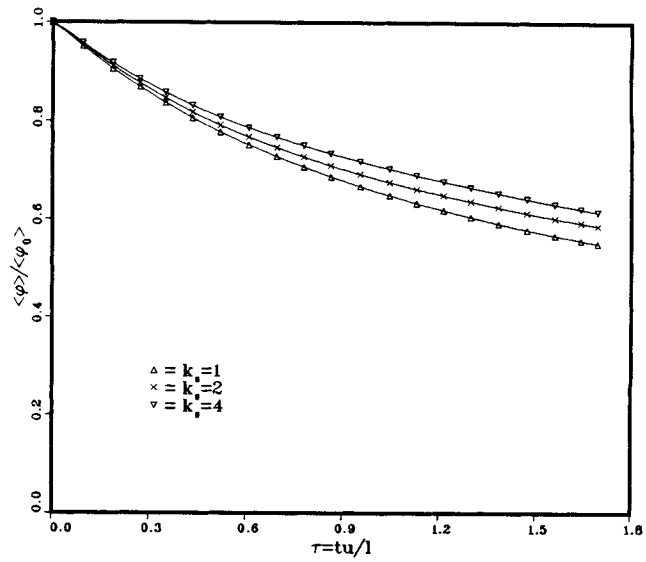

Figure 2. Evolution of means for scalar fields with different initial length scales in moderate (*Da* = 0.3) second-order reactions.

Runs *v1pd-s1*, *s2* and *s4*.

$$A + B \xrightarrow{c_1} D$$
$$A + D \xrightarrow{c_2} P.$$

The source term for each species can be written as:

$$S_a = -c_1\phi_a\phi_b - c_2\phi_a\phi_d, \quad S_b = -c_1\phi_a\phi_b \tag{11}$$

$$S_d = c_1\phi_a\phi_b - c_2\phi_a\phi_d, \quad S_p = c_2\phi_a\phi_d. \tag{12}$$

By substituting Eqs. 11 and 12 into Eq. 3 and utilizing the homogeneous conditions, it can be easily shown that

$$\langle\phi_b\rangle + \langle\phi_d\rangle + \langle\phi_p\rangle = \langle\phi_{b0}\rangle \tag{13}$$

$$\langle\phi_a\rangle - \langle\phi_b\rangle + \langle\phi_p\rangle = \langle\phi_{a0}\rangle - \langle\phi_{b0}\rangle. \tag{14}$$

In our simulations, $\langle\phi_{a0}\rangle = \langle\phi_{b0}\rangle = 0.5$, hence, we should have:

$$\langle\phi_d\rangle + \langle\phi_p\rangle = \langle\phi_{b0}\rangle - \langle\phi_b\rangle$$

and

$$\langle\phi_p\rangle = \langle\phi_b\rangle - \langle\phi_a\rangle.$$

All of our simulation results agree excellently with these relations.

A parallel/consecutive reaction is determined by three processes: the turbulent mixing, an original reaction producing an intermediate reactant, and a final reaction. Since the Damköhler numbers (chemical time scales based on $1/c_f\sqrt{\langle\phi_{a0}\rangle\langle\phi_{b0}\rangle}$) used in this research are in the range of (0.1, 10.0), a mostly low and moderate range, most reactions are controlled by the reaction rates except, perhaps, in the cases where $Da_1 \sim 10$. Da_2 is defined by $c_2\sqrt{\langle\phi_{a0}\rangle\langle\phi_{b0}\rangle}\,l/u$ in our

decay more rapidly when the initial length scales are smaller (Figure 4). This is not surprising considering that large eddies must break into smaller ones before molecular diffusion takes effect. This effect is also evident in the *s2s3* case when the initial length scale of B is smaller than that of A.

The initial correlation is shown to have little effect on the evolution of the scalar means (Figure 5). It, however, does affect the evolution of scalar variances. The variance decays more slowly for poorly correlated initial scalar fields (Figure 6).

The Damköhler number is a measure of the chemical reaction rate, and higher *Da* definitely results in faster decay of the scalar means. It, however, appears that the chemical reaction has negligible effect on the evolution of the scalar Taylor microscale, which represents the mixing length scale (Figures 7 and 8).

Consider parallel/consecutive reactions:

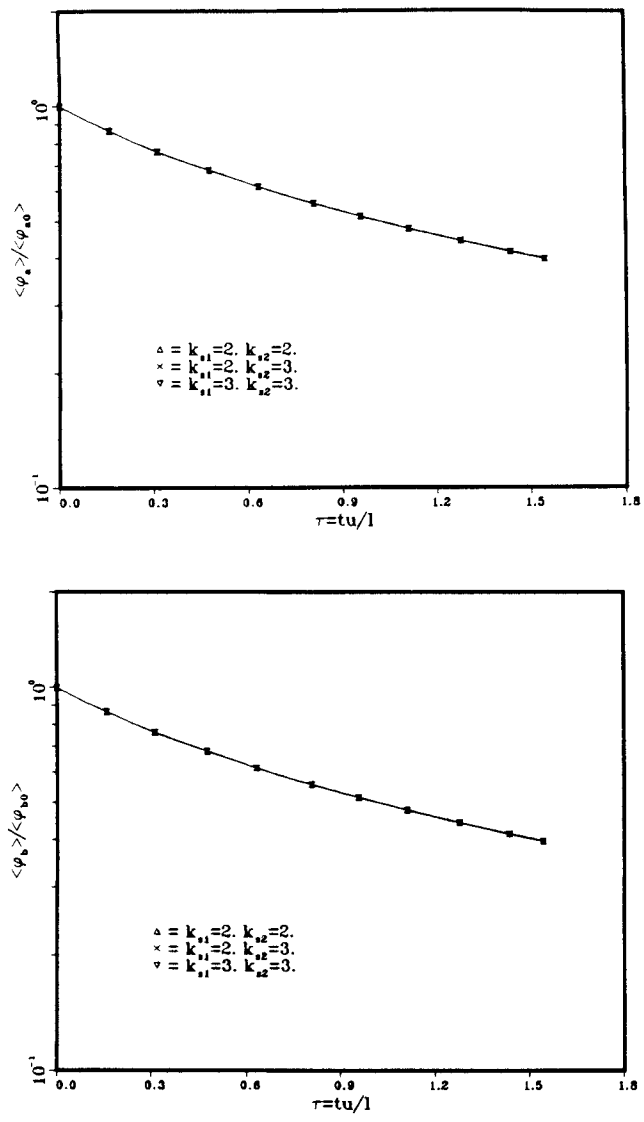

Figure 3. Evolution of scalar means $\langle\phi_a\rangle$ (upper) and $\langle\phi_b\rangle$ (lower).

Da = 1.0. Runs *v3pb*: *s2s2*, *s2s3*, *s3s3*.

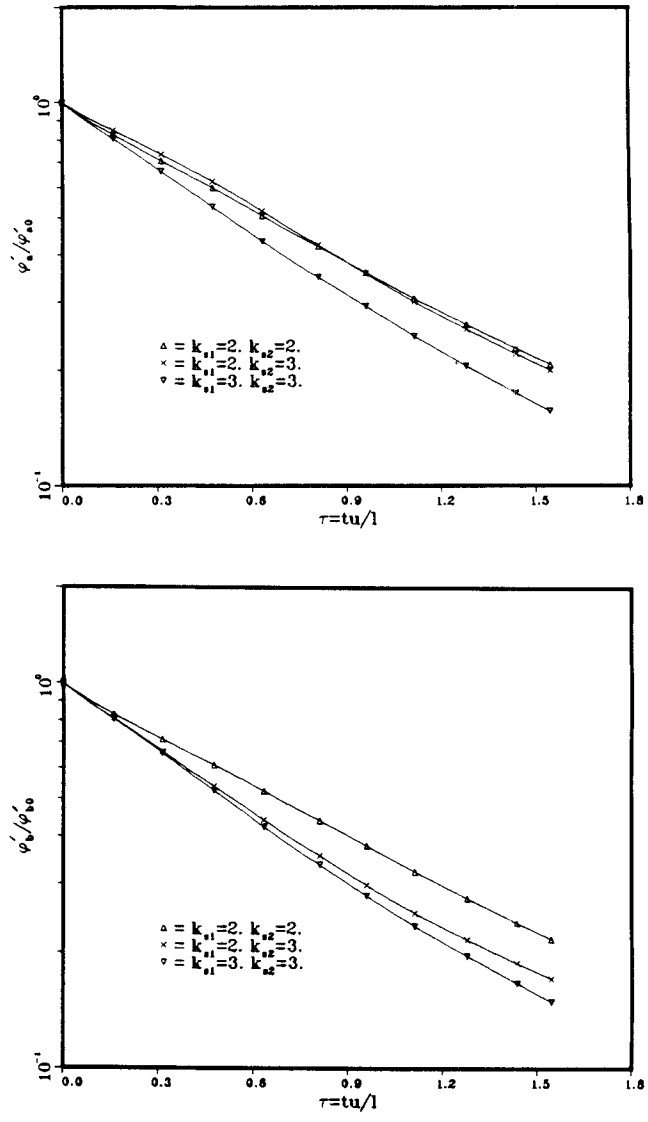

Figure 4. Evolution of scalar variances $\langle\phi'_a\rangle$ (upper) and $\langle\phi'_b\rangle$ (lower).

Da = 1.0. Runs *v3pb*: *s2s2*, *s2s3*, *s3s3*.

simulation because $\langle\phi_{d0}\rangle = 0$. Therefore, the chemical reaction rate for the second reaction is still slow even for a fairly large Da_2. In the following, we will briefly discuss the Damköhler number effects and compare them with the numerical results.

For the two reactions involved in a parallel/consecutive reaction, c_1 functions as an input threshold since it determines the production rate of ϕ_d, whose presence is necessary for the second reaction, while c_2 serves as an output threshold because, no matter how fast the first reaction is, the final production rate is determined by the second reaction. The reaction output is determined largely by the relative magnitudes of c_1 and c_2, which are represented by the corresponding Damköhler numbers Da_1 and Da_2. It is, therefore, convenient to interpret our numerical results in terms of Da_1 and Da_2/Da_1.

For the $Da_1 \gg Da_2$ case, Figure 9 shows a similar trend for the evolution of scalar means for four groups of data (Da_1, Da_2) = (10, 1; 1, 0.1; 1, 0.2; 5, 1) if time is scaled by Da_1. In fact, if the ratio Da_2/Da_1 is the same, the evolution of the scalar means is almost identical for each pair of simulations after the rescaling of time. There are, however, differences between cases with the same Da_1 but different Da_2/Da_1 of 0.1 and 0.2 (lower and upper figure, respectively). It can be expected that if Da_2/Da_1 is small enough, the scalar evolutions will be determined entirely by Da_1.

The $Da_1 \ll Da_2$ case also exhibits dependency on Da_1 and Da_2/Da_1 (Figure 10) as in the $Da_1 \gg Da_2$ case. Time again scales with Da_1.

In fact, for reaction-limited reactions, we can discuss the qualitative behavior of the scalar evolution merely by using the following chemical kinetics:

$$\frac{d\phi_a}{dt} = -c_1\phi_a\phi_b - c_2\phi_a\phi_d$$

$$\frac{d\phi_b}{dt} = -c_1\phi_a\phi_b$$

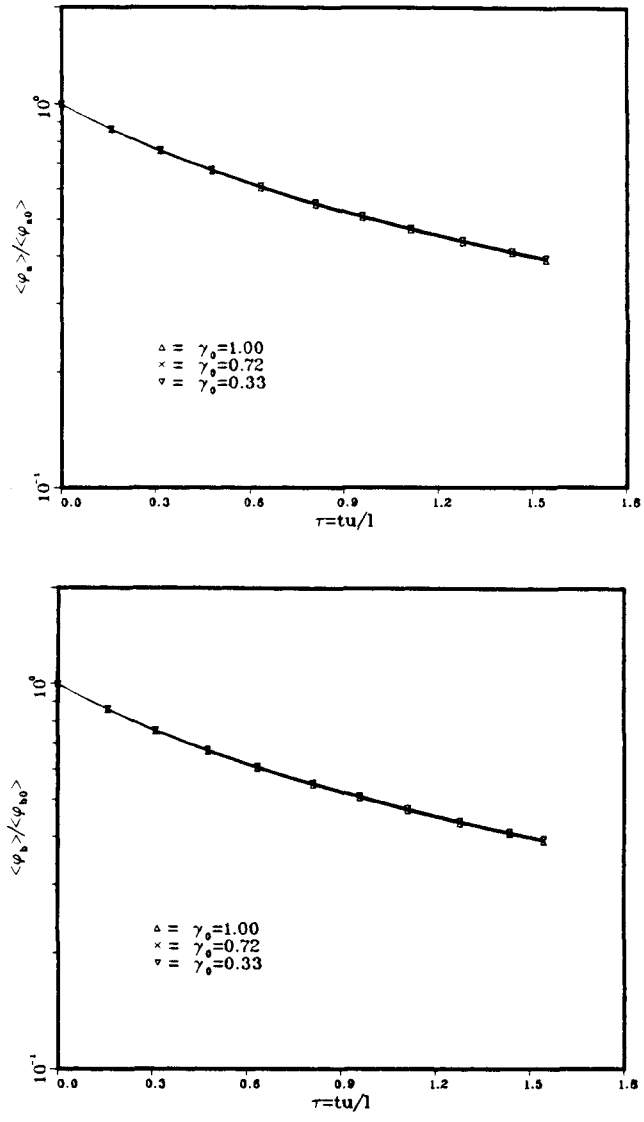

Figure 5. Evolution of scalar means for species *A* (upper) and *B* (lower) under various initial correlations.

Da = 1.0. Runs *v3pb*: *s2s2*, *s2c2*, *s2c3*.

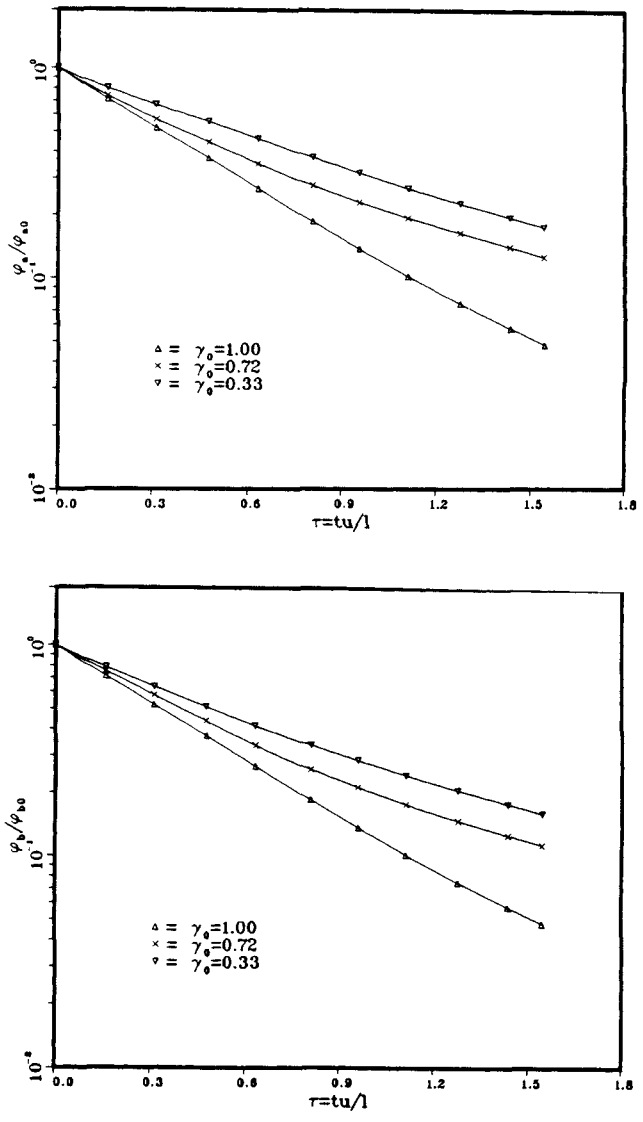

Figure 6. Evolution of scalar variances for species *A* (upper) and *B* (lower) under various initial correlations.

Da = 1.0. Runs *v3pb*: *s2s2*, *s2c2*, *s2c3*.

$$\frac{d\phi_d}{dt} = c_1\phi_a\phi_b - c_2\phi_a\phi_d$$

$$\frac{d\phi_p}{dt} = c_2\phi_a\phi_d$$

When $t = 0$, $\phi_a'/\langle\phi_a\rangle$ and $\phi_b'/\langle\phi_b\rangle$ are less than 25% in our simulations, where $\phi_a' = \sqrt{\phi_{af}^2}$, and ϕ_d and ϕ_p are both zero. Hence, to a good approximation, we can treat ϕ_a and ϕ_b as constants in the initial period and obtain the following relations ($t \ll 1$).

$$\langle\phi_d\rangle = \frac{c_1}{c_2}\langle\phi_{b0}\rangle(1 - e^{-c_2\langle\phi_{a0}\rangle t}) \approx c_1\langle\phi_{a0}\rangle\langle\phi_{b0}\rangle t$$

and

$$\langle\phi_d\rangle \approx \frac{1}{2}c_1c_2\langle\phi_{a0}\rangle^2\langle\phi_{b0}\rangle t^2.$$

Our results are consistent with this initial behavior (Figures 9 and 10).

If Da_1 is small, both ϕ_a and ϕ_b decay very slowly; hence, the above approximation is valid for a long period of time. Under this circumstance, if c_2 (Da_2) is large, ϕ_d quickly approaches to a saturated state. In other words, if the first reaction is slow but the second one is rapid, the intermediate species ϕ_d produced by the first reaction is quickly consumed by the second reaction and an equilibrium state for species ϕ_d is expected to be reached. This is indeed the case as can be seen in Figure 11. The asymptotic analysis suggests that:

$$\langle\phi_d\rangle = \frac{c_1}{c_2}\langle\phi_b\rangle = \frac{Da_1}{Da_2}\langle\phi_b\rangle.$$

However, we do not expect this asymptotic relation to be totally satisfied by the numerical results, since our simplified approximations (such as using $\langle\phi_{a0}\rangle$ to replace ϕ_a) are not valid

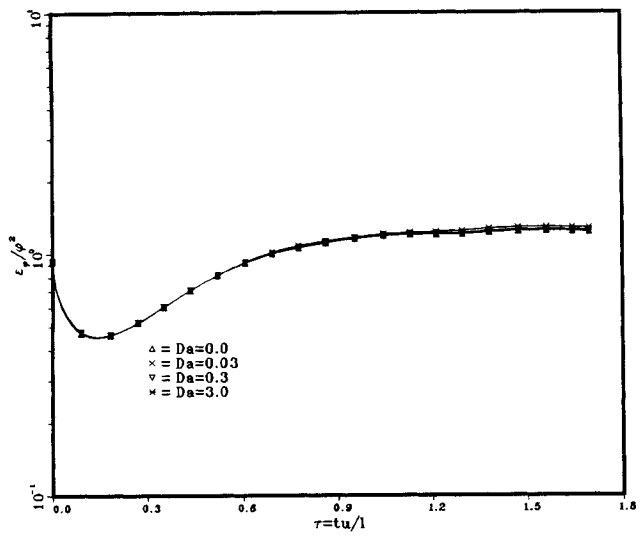

Figure 7. Evolution of scalar dissipation-to-variance ratios for second-order reactions under different reaction rates.

Initial field *v1pd-s2*.

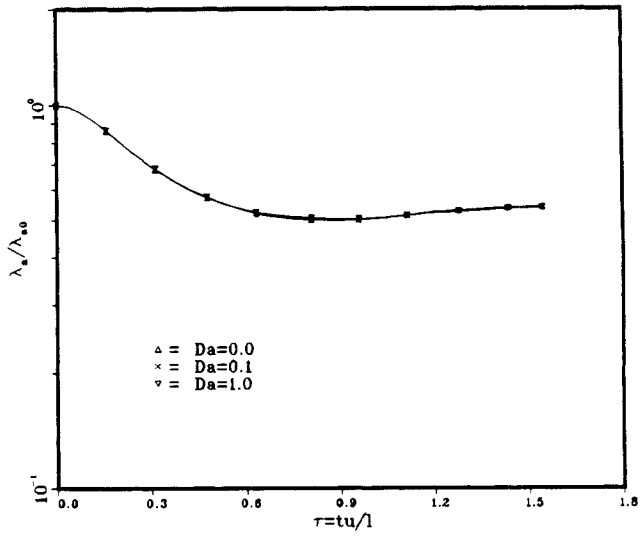

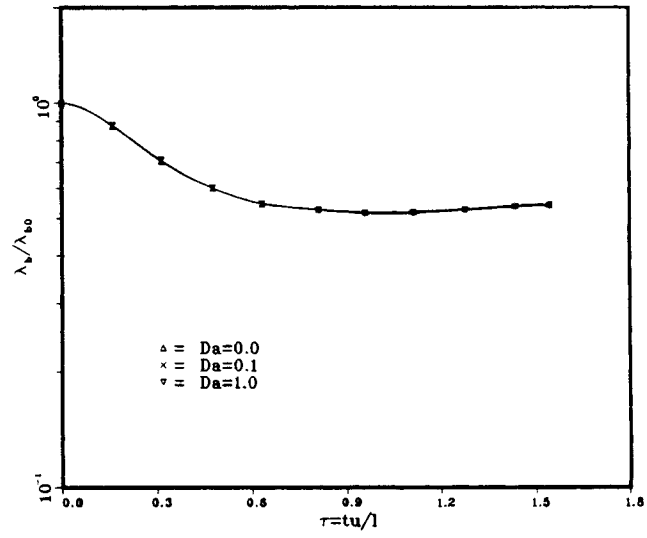

Figure 8. Evolution of Taylor scales for species *A* (upper) and *B* (lower) under various initial correlations.

Da = 1.0. Runs *v3pd*: *s2s2*.

in the later period of the scalar evolution. Nevertheless, the above simplified analysis does provide a good qualitative view.

Test of 3E closure model

Dutta and Tarbell (1989) recently proposed a three-environment (3E) and a four-environment (4E) pure-mixing asymptote models to treat parallel consecutive reactions, in which two primary reactants are from two separate feed streams, therefore they are initially segregated (Dutta and Tarbell, 1989). These models originate from the one-step, two-species reactions and were shown to produce results that agree with the experimental data.

The formulation of the 3E pure-mixing asymptote model is:

$$\overline{\phi_{af}\phi_{bf}} = -I_s(\bar{\phi}_a\bar{\phi}_{b0} + \bar{\phi}_{a0}\bar{\phi}_b - \bar{\phi}_a\bar{\phi}_b), \tag{15}$$

where I_s is identified as the segregation coefficient for the pure-mixing case (that is, there is no reaction between A and B), and $\bar{\phi}_{a0}$ and $\bar{\phi}_{b0}$ are the initial means. Again, ϕ_{af} and ϕ_{bf} represent the fluctuations of scalar fields ϕ_a and ϕ_b. This is a direct generalization of the Toor hypothesis, which states that the covariance may depend only on the hydrodynamics and not on the reaction rate (Toor, 1975; Dutta and Tarbell, 1989). If there is no reaction, it can be easily shown that Eq. 15 recovers the definition of segregation coefficient:

$$\overline{\phi_{af}\phi_{bf}} = -I_s\bar{\phi}_{a0}\bar{\phi}_{b0}$$

by noting that

$$\bar{\phi}_a = \bar{\phi}_{a0} \quad \text{and} \quad \bar{\phi}_b = \bar{\phi}_{b0}.$$

I_s is determined merely by turbulent mixing and therefore should not be affected by different reaction rates. To numerically test this model, we plot I_s calculated from numerical data for single-step reactions under different reaction rates according to Eq. 15 (Figure 12). Since it is impossible to generate homogeneous initial fields with two feed streams, we instead use two totally segregated homogeneous fields as our initial scalars. The results show that the effects of reaction on I_s are indeed negligible for moderate reaction rates, thus confirming the assumption in the 3E model.

However, careful examination of the results shows that as the reaction rate increases, the effect of reaction starts to appear, as indicated in the case of $Da = 10$. This can be understood rather easily. By starting from a totally segregated state, the initial evolutions of the scalar fields are dominated by the turbulent diffusion effect because the reaction can only happen between mixed species. After the initial period, part of the scalars become mixed, but under moderate reaction rates only a fraction of the mixed species is reacted and the diffusion effect continues to dominate the scalar cross-correlation evolution. Along this line of reasoning, it is obvious that as the reaction rate increases further, the effect of reaction on the

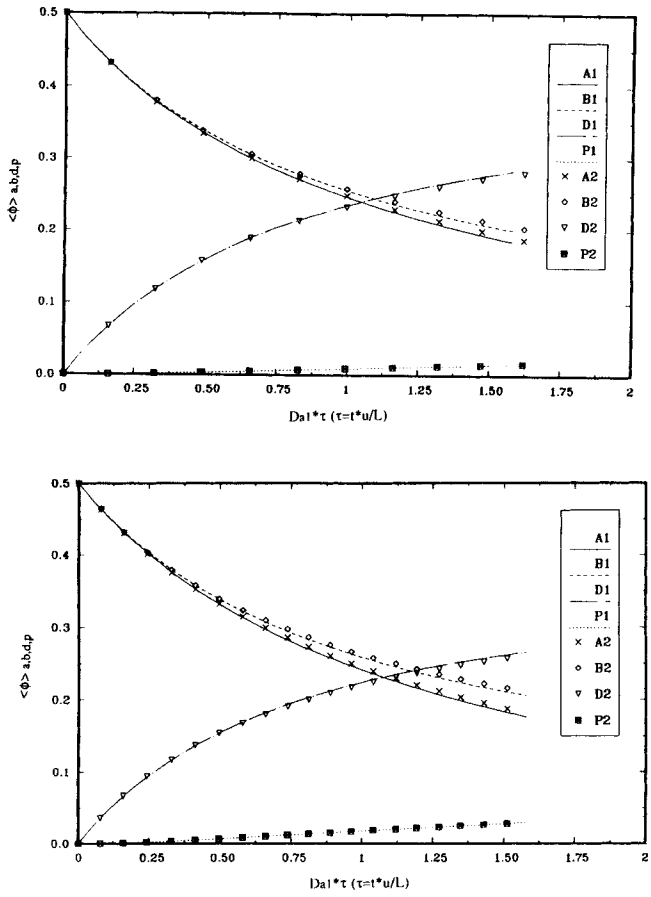

Figure 9. Evolution of scalar means in $Da_1 >> Da_2$ case.

Upper, $Da_1 = 1$, $Da_2 = 0.1$ (line) and $Da_1 = 10$, $Da_2 = 1$ (symbol); lower, $Da_1 = 1$, $Da_2 = 0.2$ (line) and $Da_1 = 5$, $Da_2 = 1$ (symbol). Run *v3pb-s2c3*.

scalar correlations becomes much more important. In fact, the situation becomes diffusion-limited. But, whereas turbulent diffusion determines the time scale as in pure mixing, the fast reaction rate may strongly influence the values of scalar cross-correlations in such a way as to negate Eq. 8. This seems to have occurred somewhat by $Da = 10$. It may never be a large

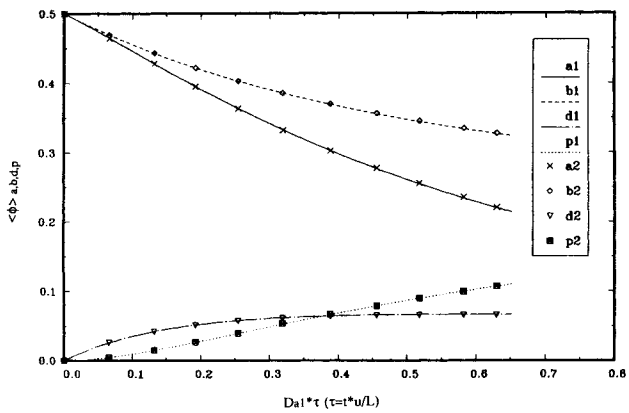

Figure 10. Evolution of scalar means in $Da_1 << Da_2$ case.

$Da_1 = 0.2$, $Da_2 = 1$ (line); $Da_1 = 1$, $Da_2 = 5$ (symbol). Run *v3pb-s2c3*.

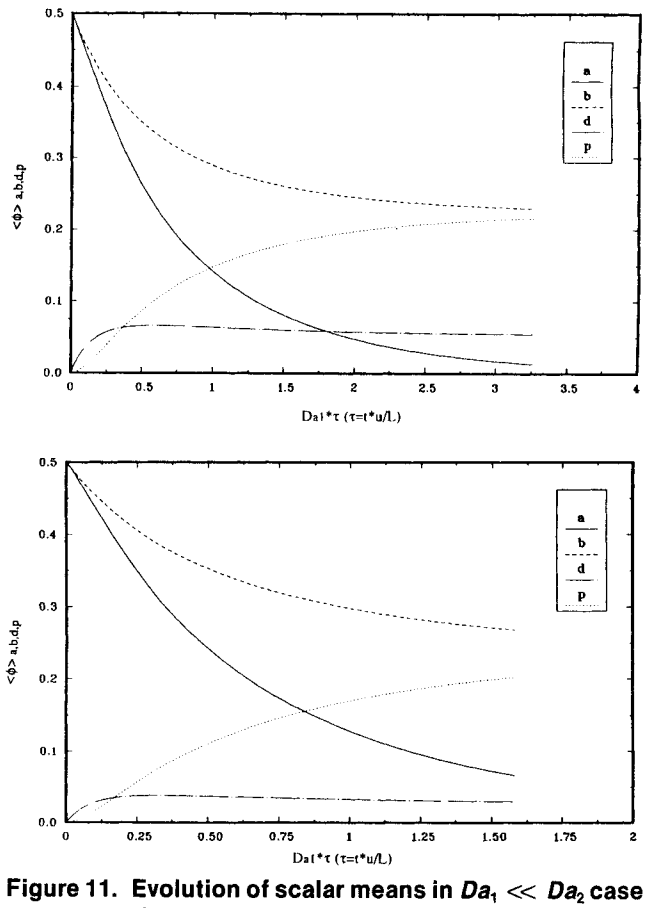

Figure 11. Evolution of scalar means in $Da_1 << Da_2$ case (for asymptotic behavior).

$Da_1 = 1.0$, $Da_2 = 5$ (upper); $Da_1 = 1$, $Da_2 = 10$ (lower). Run *v3pb-s2c3*.

effect since the time scale remains the turbulent diffusion time when Da is large.

As a matter of fact, it can be shown that Eq. 15 does not recover the limiting form

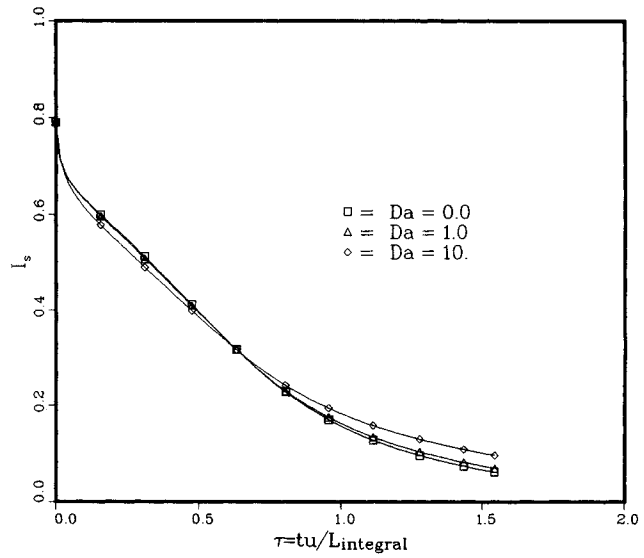

Figure 12. Evolution of I_s for one-step simple reaction under different reaction rates.

Run *v3pb-s2s2*.

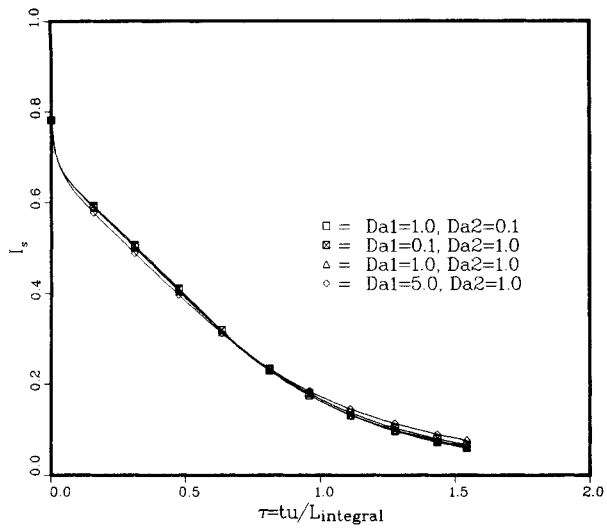

Figure 13. Evolution of I_s for the first reaction in the parallel/consecutive reaction scheme under different reaction rates.

Run *v3pb-s2s3*.

$$\overline{\phi_{af}\phi_{bf}} = -\bar{\phi}_a\bar{\phi}_b$$

for infinitely fast reactions. This can be demonstrated in the following. According to Dutta and Tarbell (1989),

$$\bar{\phi}_a = I_s\bar{\phi}_{a0} \quad \text{and} \quad \bar{\phi}_b = I_s\bar{\phi}_{b0} \tag{16}$$

for infinitely fast reactions, where I_s is the segregation coefficient for the pure-mixing case and is a function of time varying from 1 (totally segregated initial state) to 0 (totally mixed final state). Substituting Eq. 16 into Eq. 15, it is clear that the form for the infinitely fast reaction limit is not satisfied unless $I_s = 1$, which is true only at the initial stage. Therefore, the 3E pure-mixing asymptote model may not be valid for fast reactions.

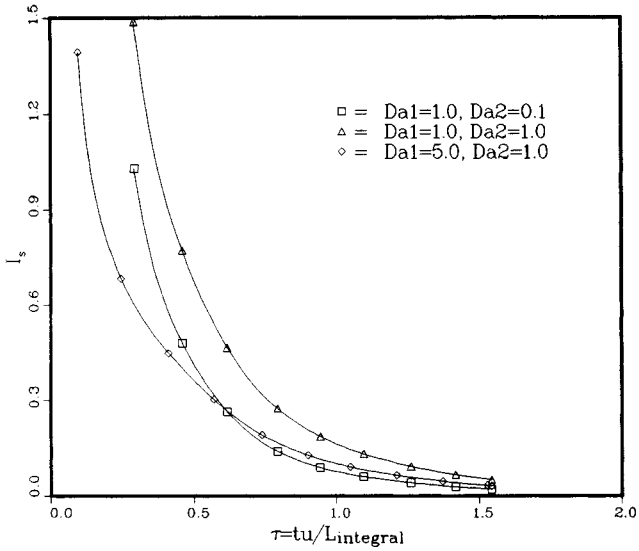

Figure 14. Evolution of I_s for the second reaction.

Same run as in Figure 13.

The effect of chemical reaction can be demonstrated by applying the 3E pure-mixing asymptote model to parallel/consecutive reactions. The model equations suggested by Dutta and Tarbell (1989) are:

$$\overline{\phi_{af}\phi_{bf}} = -I_s(\bar{\phi}_a\bar{\phi}_{b0} + \bar{\phi}_{a0}\bar{\phi}_b - \bar{\phi}_a\bar{\phi}_b) \tag{17a}$$

$$\overline{\phi_{af}\phi_{df}} = -I_s\bar{\phi}_d(\bar{\phi}_{a0} - \bar{\phi}_a), \tag{17b}$$

where the model equation for the second reaction is obtained by noting that $\bar{\phi}_{d0} = 0$. The DNS results are employed to calculate I_s according to Eq. 17.

Figure 13 shows the values of I_s obtained from Eq. 17*a* while Figure 14 displays those calculated from Eq. 17*b*. Reaction rates for both reactions are moderate. It is clear that Figure 13 reproduces Figure 12, indicating that only a very small amount of ϕ_a is involved in the reactions and the dominant effect remains diffusion for ϕ_a and ϕ_b. However, from Figure 14, strong dependence of I_s on the reaction rate is observed. This is not very surprising since ϕ_d is generated by the first reaction; therefore, the amount ϕ_d available for the second reaction depends on the reaction rate of the first one. Also ϕ_d is produced by a reaction between ϕ_a and ϕ_b so that ϕ_d and ϕ_a are not segregated. The dominant effect in the second reaction is, therefore, not diffusive mixing, but instead it is the direct reaction between ϕ_a and ϕ_d.

Dutta and Tarbell also suggested a 4E model that slightly modifies the 3E model. In the 4E model,

$$\overline{\phi_{af}\phi_{bf}} = -I_s(\bar{\phi}_a\bar{\phi}_{b0} + \bar{\phi}_{a0}\bar{\phi}_b - \bar{\phi}_a\bar{\phi}_b) + I_s^2(I_s - 1)\bar{\phi}_a\bar{\phi}_b$$

$$\overline{\phi_{af}\phi_{df}} = -I_s\bar{\phi}_d(\bar{\phi}_{a0} - \bar{\phi}_a) + I_s^2(I_s - 1)\bar{\phi}_a\bar{\phi}_d.$$

It is easily seen that the difference between 4E and 3E is a term with a coefficient $I_s^2(I_s - 1)$. It has been shown that the 3E and 4E models produce almost identical results (Dutta and Tarbell, 1989). No attempt has been made to test this model against DNS data in the current work. However, a simple observation can be made about the model equations. In the limit of no reaction, the model equation should recover the definition for the segregation coefficient as was shown for the case of the 3E model. This is not true for the 4E pure-mixing asymptote model.

Selectivity

One of the interesting features of the parallel-consecutive reaction scheme is selectivity, which we define, following Bourne (Bourne et al., 1981; Bourne, 1990), by

$$X_s = \frac{2\bar{\phi}_p}{\bar{\phi}_d + 2\bar{\phi}_p},$$

where $\bar{\phi}_d$ is the mean concentration of the desired product D while $\bar{\phi}_p$ is that of the by-product P. X_s is zero for perfect selectivity and unity when only P is obtained. The computations we have carried out for selectivity are for a single set of turbulence parameters (run v3) with several nonzero Damköhler numbers for each of the two reactions.

The results are plotted in Figure 15. As the ratio of Damköhler numbers, Da_1/Da_2, increases from 0.1 to 10.0, the selectivity of D improves monotonically as expected. Similar results have also been obtained by other researchers (Chak-

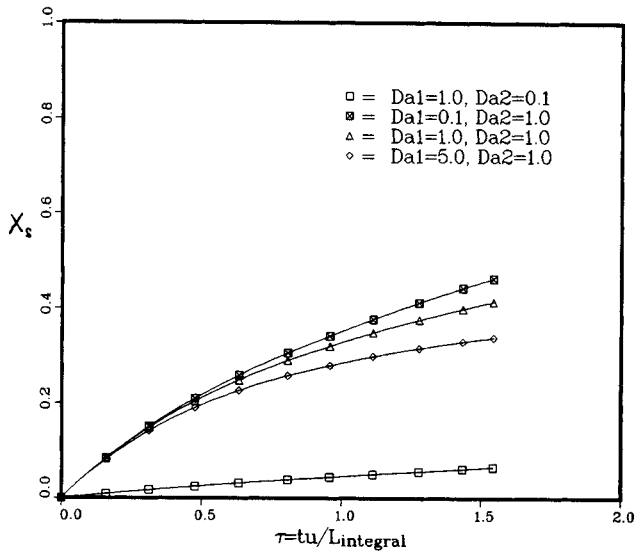

Figure 15. Evolution of X_s under different Damköhler numbers.

Same run as in Figure 13.

rabarti and Hill, 1990). For a range of Da_1 from 0.1 to 5.0, with $Da_2 = 1.0$, the selectivity is not dramatically affected. On the other hand, when Da_1 is fixed at 1.0, there is a significant decrease in X_s when Da_2 is reduced from 1.0 to 0.1. Various turbulence parameters, such as length scales and energy and vorticity intensity, can be investigated for their influence on selectivity. Some results have been reported by Chakrabarti and Hill (1990). This aspect of the DNS computations will be explored next, whose results are expected to be a valuable data set. Reactive flow models can deal with higher Reynolds and Schmidt numbers than DNS.

Conclusion

A numerical experiment has been conducted on chemically reactive flows involving multispecies reactions as well as multistep reaction schemes. The DNS technique provides an effective tool to investigate complicated reaction problems by isolating the effects of different parameters. As was pointed out earlier, the power of the DNS is highly restricted by the capabilities of available computers. For this reason, it cannot, in the foreseeable future (Reynolds, 1989), be directly applied to calculate practical problems, such as those of high Reynolds numbers and/or with complicated flow geometry.

The DNS method is recommended to be used to test empirical models that can be applied to more practical situations. Examples of doing this are demonstrated in this article. The three-environment pure-mixing asymptote model, recently suggested by Dutta and Tarbell (1989), can be applied to one-step simple reactions between two initially segregated species under moderate chemical reactions, but it may not apply to all reaction cases. Selectivity can also be examined in depth as discussed previously. More simulations with a wider set of turbulence parameters should be performed to better assess the available empirical models, such as those suggested by Heeb and Brodkey (1990).

Acknowledgment

We would like to thank Dr. V. Eswaran and Prof. S. B. Pope for providing us with the original program for this study. We gratefully acknowledge the support for this research from the National Science Foundation under grant CTS-8706249. Part of the computation was carried out in the Cornell National Supercomputer Facility, which is supported in part by the National Science Foundation, the State of New York, and the IBM Corporation.

Notation

A, B, D, P = chemical species
Da = Damköhler number
$D_{\phi i}$ = diffusivity for scalar i
E, E_ϕ = velocity and scalar spectrum
I_s = segregation coefficient
$\hat{L}, \hat{L}_N$ = operator and its projection in N-dimensional subspace
S_a = reaction source term for species A
X_s = selectivity
c_i = reaction rate
f, g = functions of space and time
$\tilde{f}$ = space Fourier transform of f
$f(j)$ = value of f at grid point j
$\vec{f}, f_1, f_2, f_3$ = forcing terms in the Navier-Stokes equations
$\tilde{f}(k)$ = kth Fourier mode of f
k, k_s = wave numbers
l, l_ϕ = integral length scales of velocity and scalar fields
u, v, w = velocity components
v_j = same as u, v, w for $j = 1, 2, 3$
$\vec{v}$ = (v_1, v_2, v_3)
x, t = space and time coordinates
ϵ, ϵ_ϕ = velocity and scalar dissipation rates
ϕ_j = concentration of species j
ϕ_{i0} = initial concentration of ϕ_i
ϕ_{if} = concentration fluctuation of species i
λ, λ_ϕ = Taylor microscales of velocity and scalar fields
η = Kolmogorov microscale
θ = random angle
ν = fluid viscosity
$\langle a \rangle, \bar{a}$ = mean expected value of a

Literature Cited

Bourne, J. R., F. Kozicki, and P. Rys, "Mixing and Fast Chemical Reaction: I. Test Reactions to Determine Segregation," *Chem. Eng. Sci.*, **36**, 1643 (1981).

Bourne, J. R., "Turbulent Mixing and the Selectivity of Fast Chemical Reactions," *IUTAM Symp. on Fluid Mech. of Stirring and Mixing*, La Jolla, CA (1990).

Chakrabarti, M., and J. C. Hill, "Direct Numerical Simulation of Chemical Selectivity in Turbulent Flows," *Symp. on Turbulence*, Rolla, MO (1990).

Corrsin, S., "Statistical Behavior of a Reacting Mixture in Isotropic Turbulence," *Phys. Fluids*, **1**, 42 (1958).

Dutta, A., and J. M. Tarbell, "Closure Models for Turbulent Reacting Flows," *AIChE J.*, **35**, 2013 (1989).

Eswaran, V., and S. B. Pope, "An Examination of Forcing in Direct Numerical Simulations of Turbulence," *Comp. & Fluids*, **16**, 257 (1988a).

Eswaran, V., and S. B. Pope, "Direct Numerical Simulations of the Turbulent Mixing of a Passive Scalar," *Phys. Fluids*, **31**, 506 (1988b).

Gao, F., "Theoretical and Numerical Investigations of Scalar Fields in Isotropic Turbulence," PhD Thesis, State University of New York at Stony Brook (1990).

Givi, P., and P. A. McMurtry, "Nonpremixed Reaction in Homogeneous Turbulence: Direct Numerical Simulation," *AIChE J.*, **34**, 1039 (1988).

Gottlieb, D., and S. A. Orszag, *Numerical Analysis of Spectral Methods*, SIAM (1977).

Heeb, T. E., and R. S. Brodkey, "Turbulent Mixing with Multiple Second-Order Chemical Reactions," *AIChE J.*, **36**, 1457 (1990).
Hinze, J. O., *Turbulence*, 2nd ed., McGraw-Hill (1975).
Hussaini, M. Y., and T. A. Zang, "Spectral Methods in Fluid Dynamics," *Ann. Rev. Fluid Mech.*, **19**, 339 (1987).
Leonard, A. D., and J. C. Hill, "Direct Numerical Simulation and Simple Closure Theory for a Chemical Reaction in Homogeneous Turbulence," *Turbulent Reactive Flows*, R. Borghi and S. N. B. Murthy, eds, Springer-Verlag (1989).
Leonard, A. D., and J. C. Hill, "Kinematics of the Reaction Zone in Homogeneous Turbulence," *Proc. Symp. on Turbulence*, Rolla, MO (1990).
O'Brien, E. E., "On the Statistical Behavior of a Dilute Reactant in Isotropic Turbulence," PhD Thesis, Johns Hopkins University (1960).
Patterson, G. S., and S. A. Orszag, "Spectral Calculations of Isotropic Turbulence: Efficient Removal of Aliasing Interactions," *Phys. Fluids*, **14**, 2538 (1971).
Reynolds, W. C., "The Potential and Limitations of Direct and Large Eddy Simulations," *Whither Turbulence*, J. L. Lumley, ed., Springer-Verlag (1990).
Riley, J. J., R. W. Metcalfe, and S. A. Orszag, "Direct Numerical Simulation of Chemically Reacting Turbulent Mixing Layers," *Phys. Fluids*, **29**, 406 (1986).
Rogallo, R. S., "Numerical Experiments in Homogeneous Turbulence," NASA TM-81315 (1981).
Toor, H. L., "The Non-premixed Reaction: A + B → Products," *Turbulence in Mixing Operations*, R. S. Brodkey, ed., Academic Press, New York (1975).

Manuscript received Feb. 1, 1991, and revision received Aug. 5, 1991.